JOURNAL OF SOLID STATE CHEMISTRY 77, 170–179 (1988)

Concerning the Intersecting Tunnel Structure of a Novel Vanadyldiphosphate $K_2(VO)_3(P_2O_7)_2$ and Its Structural Relationships with Other V(V) and V(IV) Phosphates and Relatives

A. LECLAIRE, H. CHAHBOUN, D. GROULT, AND B. RAVEAU

Laboratoire de Cristallographie et Sciences des Matériaux (CRISMAT), ISMRa, Bd du Maréchal Juin, 14032 Caen Cedex, France

Received April 21, 1988; in revised form July 6, 1988

$K_2V_3P_4O_{17}$, $Mr = 626.91$, orthorhombic, $Pna21$, $a = 17.407(1)$, $b = 11.3438(7)$, $c = 7.2964(15)$ Å, $V = 1440.8(5)$ Å^3, $Z = 4$, $D_x = 2.89$ Mg m^{-3}, $\lambda(MoK\alpha) = 0.71073$ Å, $\mu(MoK\alpha) = 2.96$ mm^{-1}, $F(000) = 1212$, $T = 293$ K, $R = 0.049$, and $R_w = 0.055$ for 574 independent observed reflections with $I \geq 3\sigma(I)$. The host lattice $[V_3P_4O_{17}]$ is built up from corner-sharing VO_6 octahedra, VO_5 square pyramids, and PO_4 tetrahedra. The structure can be described in terms of mixed chains $[V_2P_8O_{30}]_\infty$ linked through $[V_2O_{10}]$ units. The $[V_2P_8O_{30}]_\infty$ chains are formed of ReO_3-type chains connected to diphosphate groups whereas the $[V_2O_{10}]$ units are formed from one corner-shared VO_6 octahedron and one VO_5 pyramid. The framework delimits intersecting tunnels running along c and b which suggest possible ion exchange properties. The ability of V(IV) to form a short vanadyl bond VO^{2+} is observed in all the vanadium polyhedra leading to the formula $K_2(VO)_3(P_2O_7)_2$. A comparison of the structure with that of different V(IV) and V(V) phosphates and related compounds is carried out.

Introduction

Vanadium phosphorus oxides are used as heterogeneous catalysts in various organic reactions, such as the mild oxidation of butenes (*1*) or butane (*2*) to maleic anhydride. The redox mechanism occurring during catalysis results from the ability of vanadium to exist in several oxidation states, and a variety of coordinations. This oxidation catalysis depends on the crystal structure of those mixed frameworks, and their structural analysis is very important in understanding the mechanism of the catalytic reaction. Moreover such mixed frameworks, involving d^n transition ions are susceptible to present interesting physical properties. For this reason, the investigation of the system V–P–Si–O was recently carried out leading to the V(III) silicophosphate $V_3P_5SiO_{19}$ (*3*). In an attempt to synthesize new mixed frameworks involving phosphorus and vanadium, the K–V–P–O system was investigated. The present work deals with the crystal structure determination of a new diphosphate of V(IV) $K_2V_3P_4O_{17}$ and with its relationships to other mixed frameworks involving vanadium and phosphorus.

Experimental

Powder synthesis. The starting materials K_2CO_3, $(NH_4)_2HPO_4$, and V_2O_5 were AR quality. They were thoroughly mixed in an agate mortar in the appropriate ratios 4 : 8 : 3. The mixture was then heated 1 hr at

0021-4596/88 $3.00

600°C in an platinum crucible in air in order to eliminate CO_2, NH_3, and H_2O. After cooling the amount of V_2O_3 or metallic vanadium required for the reduction of vanadium (V) into vanadium (IV) was added with the reaction product. The mixture was homogeneized by grinding and introduced into a platinum tube which was placed in an evacuated silica ampoule. The reaction mixture was heated for 5 days at 550°C. After quenching at room temperature, a greenish slightly sintered powder was obtained.

Single crystal growth. Single crystals were grown in the following way: approximately 500 mg of β-$VOPO_4$, prepared by conventional methods (*4*), was introduced in a platinum crucible containing traces of K_2O. Such traces were obtained by fusing $KHSO_4$ in the platinum crucible, short leaching in hot water, and heating at 800°C. The reaction mixture was placed in an evacuated silica ampoule and heated for 5 days at 550°C. The crystals grew on the walls of the platinum tube in the form of green needles with a rectangular section.

X-ray analysis. The cell parameters were determined from the single crystal X-ray diffraction study. They allowed the X-ray powder diffraction pattern to be indexed correctly, except for very weak extra lines which correspond to the V(III) diphosphate KVP_2O_7 isotypic to $KMoP_2O_7$ (*5*). This is easily explained by the low stability of the oxide $K_2(VO)_3(P_2O_7)_2$. Further heating at 600°C led indeed to the formation of a great amount of KVP_2O_7.

Structure: Determination and Refinement

Unit cell parameters were determined by least-squares refinement of the setting angles for 25 reflections [$3° < \theta(\text{Mo}K\alpha) < 17°$] automatically centered on an Enraf-Nonius CAD-4 diffractometer. Intensity data were recorded on the same instrument with the experimental conditions given in Table I. The data were corrected for Lorentz and polarization effect but no absorption correction was applied. Scattering factors and anomalous dispersion were taken from the International Tables for X-ray Crystallography (*6*).

TABLE I

EXPERIMENTAL DATA

Crystal form and size	Green needle, 0.024 × 0.032 × 0.312 mm
θ_{max}	45°
Index range: h	0 23
k	0 19
l	0 14
Scan type	$\omega - \theta$
Scan angle	$0.9 + 0.35 \tan \theta$
Counter slit aperture	$1 + \tan \theta$
Monochromator	Graphite
Number of hkl with $I \geq 3\sigma(I)$	574
Number of refined parameters	104
R	0.049
R_w	0.055
Δ/σ_{max}	0.5
$\delta\rho_{max}$	3 e^- Å^{-3}

The structure determination was first carried out in the centrosymmetrical *Pnam* space group consistent with the observed systematic extinctions. The atomic coordinates of vanadium and potassium were deduced from the Patterson function. The remaining atoms were located by subsequent Fourier series. The refinement of the atomic coordinates and isotropic thermal factors was carried out by the full-matrix least-squares method and unit weights. This led to thermal factors often greater than 4 Å^2 which indicated that some atoms were shifted to some extent from a mirror plane (V(1) and V(2)) and the symmetry center (V(3)). As a consequence, the refinement was performed, in a second step, in the noncentrosymmetric space group $Pna2_1$. Having raised the constraints for the atomic coordinates of vanadium, smaller values for the isotropic thermal parameters were obtained. However, nega-

TABLE II
ATOMIC PARAMETERS

Atom	X	Y	Z	B_{iso}
V(1)	0.1005(2)	0.6612(3)	0.2500(0)	0.57(6)
V(2)	0.1901(2)	0.3392(3)	0.2692(19)	0.72(7)
V(3)	0.0013(4)	0.0017(6)	0.0412(14)	0.89(7)
K(1)	0.1728(4)	0.1371(6)	0.7612(37)	3.16(14)
K(2)	0.3619(5)	0.0352(7)	0.2418(31)	4.31(21)
P(1)	0.3247(10)	0.3886(15)	−0.0430(29)	0.97(28)
P(2)	0.3285(10)	0.3916(14)	−0.4435(32)	0.97(27)
P(3)	0.0297(8)	0.2898(14)	0.0511(26)	0.67(21)
P(4)	0.0258(8)	0.2936(14)	0.4589(25)	0.67(23)
O(1)	0.1534(8)	0.5488(13)	0.2773(48)	0.83(28)
O(2)	0.1560(14)	0.7569(23)	0.4344(40)	1.03(49)
O(3)	0.1436(14)	0.7662(22)	0.0641(44)	1.03(51)
O(4)	0.0273(16)	0.6255(25)	0.4630(37)	0.99(44)
O(5)	0.0177(16)	0.6289(25)	0.0933(37)	0.99(51)
O(6)	0.1093(19)	0.3465(25)	0.0540(57)	1.11(56)
O(7)	0.1092(19)	0.3299(25)	0.4523(52)	1.11(58)
O(8)	0.2638(12)	0.4137(20)	0.4163(33)	0.72(39)
O(9)	0.2216(10)	0.2074(16)	0.2410(59)	2.27(42)
O(10)	0.2504(11)	0.4086(19)	0.0433(38)	0.72(35)
O(11)	0.0327(13)	0.1702(24)	−0.0117(37)	0.76(47)
O(12)	0.0071(14)	0.0095(20)	0.2699(64)	3.96(56)
O(13)	−0.0181(13)	−0.1649(23)	0.0486(45)	0.76(38)
O(14)	−0.1101(14)	0.0328(22)	0.0604(40)	1.38(40)
O(15)	0.1112(14)	−0.0263(22)	0.0309(43)	1.38(45)
O(16)	−0.0078(8)	0.2921(13)	0.2483(53)	1.18(30)
O(17)	0.3022(12)	0.4297(19)	−0.237(12)	3.87(47)

tive correlations occurred between the B values of independent atoms which were equivalent by a mirror plane in the centrosymmetrical *Pnam* space group. For the atomic pairs located on both sides of this pseudo-mirror plane in the $Pna2_1$ group, it was observed during the structure refinement that if one of the two isotropic B factors increased, the second one decreased and could be negative. To eliminate such an effect, subsequent refinement cycles were carried out using the average of their B values obtained from the previous cycles from each of the correlated atoms. The thermal parameters were refined isotropically since anisotropic refinement allowed for only two reflections per parameter. The final stage of refinement led to $R = 0.049$, $R_w = 0.055$ and to the parameters of the Table II.[1]

[1] Lists of structure factors are available on request from the authors.

Description of the Structure: Structural Relationships

The host lattice of this vanadophosphate (Figs. 1 and 2) is built up from corner-sharing VO_6 octahedra, VO_5 square pyramids, and disphosphate groups P_2O_7. This mixed framework delimits intersecting tunnels running along b and c, where the potassium ions are located.

The three crystallographically independent vanadium atoms are in the +4 oxidation state. The atoms V(1) exhibit a square pyramidal coordination. In those polyhedra the vanadium atoms are displaced from the basal plane formed by the oxygen atoms by 0.463, 0.465, and 0.082 Å for V(1), V(2), and V(3), respectively. Consequently, very short apical vanadium–oxygen bonds are observed: 1.585, 1.606, and 1.674 Å for (V(1–O(1), V(2)–O(9), and V(3)–O(12), respectively (Table III). These short V–O distances can be interpreted as the result of

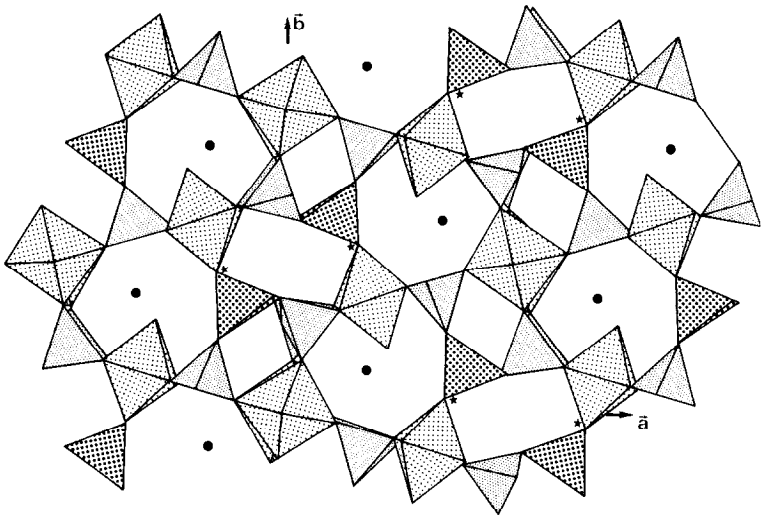

FIG. 1. Projection of the $K_2(VO)_3(P_2O_7)_2$ structure on to the (*ab*) plane showing the pseudo-rectangular tunnels and the "snail-shell-shaped" tunnels running along *c*.

the ability of V(IV) to form a vanadyl ion VO^{2+}, leading to the formulation of $K_2(VO)_3(P_2O_7)_2$. Such V–O bonds are indeed observed in several mixed frameworks containing V(IV): 1.59 Å in VO SiP_2O_8 (*7*), β-$VOSO_4$ (*8*), and $VO(PO_3)_2$ (*9*), 1.62 Å in α-$VOSO_4$ (*10*), 1.68 Å in $VOMoO_4$ (*11*), and $(VO)_2P_2O_7$ (*12*). This ability of V(IV) to form a short V=O bond can be compared to that of Mo(V) which also exhibits a d^1 configuration. $MoPO_5$ (*13*) and $K_4Mo_8P_{12}O_{52}$ (*14*) also show similar MoO_6 octahedra characterized by a molybdenyl Mo=O bond of 1.66 Å. Nevertheless, it is worth pointing out that the "MO_6" octahedra are almost regular in the Mo(V) oxides,

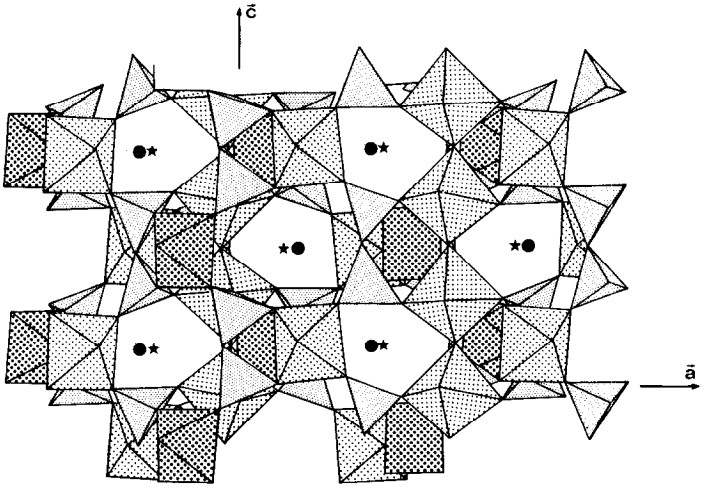

FIG. 2. Projection of the $K_2(VO)_3(P_2O_7)_2$ structure on to the (*ac*) plane showing the tunnels running along *c*.

TABLE III

INTERATOMIC DISTANCES (Å) AND BOND ANGLES (°) IN THE $V(1)O_5$, $V(2)O_6$, AND $V(3)O_6$ POLYHEDRA

V(1)	O(1)	O(2)	O(3)	O(4)	O(5)
O(1)	1.59(2)	2.63(3)	2.92(4)	2.72(4)	2.87(3)
O(2)	94(1)	1.98(3)	2.71(4)	2.70(4)	3.76(4)
O(3)	111(1)	87(1)	1.96(3)	3.89(4)	2.70(4)
O(4)	96(1)	84(1)	152(1)	2.05(3)	2.70(4)
O(5)	111(1)	154(1)	89(1)	87(1)	1.88(3)

V(2)	O(1)	O(6)	O(7)	O(8)	O(9)	O(10)
O(1)	2.46(2)	2.92(4)	2.90(4)	2.66(3)	4.06(5)	2.88(3)
O(6)	79(1)	2.11(4)	2.91(6)	3.85(4)	2.86(4)	2.56(4)
O(7)	81(1)	92(1)	1.94(4)	2.87(4)	2.85(4)	3.97(4)
O(8)	74(1)	150(1)	97(1)	1.88(2)	2.77(3)	2.73(4)
O(9)	172(2)	100(1)	107(1)	105(1)	1.61(2)	2.75(4)
O(10)	78(1)	75(1)	157(1)	86(1)	94(1)	2.11(3)

V(3)	O(11)	O(12)	$O(12^i)$	O(13)	O(14)	O(15)
O(11)	2.03(3)	2.78(4)	2.68(4)	3.93(4)	2.98(3)	2.63(4)
O(12)	97(1)	1.67(5)	3.66(4)	2.59(5)	2.56(4)	2.55(5)
$O(12^i)$	84(1)	179(4)	1.99(5)	2.70(5)	2.82(5)	2.81(5)
O(13)	169(1)	92(1)	87(1)	1.92(3)	2.76(4)	2.75(4)
O(14)	96(1)	89(1)	91(1)	90(1)	1.98(3)	3.92(4)
O(15)	83(1)	89(1)	91(1)	91(1)	178(1)	1.94(3)

Note. The diagonal indicates the M–O bond length (Å). The values above the diagonal are the O . . . O lengths (Å) and the values below are the O–M–O angles (°).

the molybdenum ion being off centered, whereas they are generally more distorted in the V(IV) oxides as shown here for $K_2V_3P_4O_{17}$ (Table III). However, the d^1 electronic configuration cannot be considered as the only factor governing the existence of short V=O bonds since a similar behavior is observed in various V(V) oxides. α-VPO_5 (*15*), β-VPO_5 (*16*), and $VAsO_5$ (*17*) have their VO_6 octahedra characterized by similar short V=O bonds of 1.58, 1.59, and 1.59 Å, respectively. The ability of V(IV) and V(V) to form a very short V=O bond induces the formation of VO_5 pyramids confirmed in $K_2V_3P_4O_{17}$ by the existence of the $V(1)O_5$ square pyramid. The pyramidal coordination of vanadium has indeed been observed up to the present only in mixed valence vanadium oxides $Cs_2V_5O_{13}$ (*18*) and $K_2V_3O_8$ (*19*), in vanadium bronzes $A_xV_2O_5$ (*20*) and $Li_{1+x}V_3O_8$ (*21*), and in the V(V) oxide V_2O_5 (*22*). The V(1)–O(1) distance (1.585 Å) observed in the pyramid $V(1)O_5$ is rather close to that observed in the other vanadium oxides whereas the V–O bonds of the basal plane $\langle V\text{–}O\rangle$ = 1.97 Å is close to those observed in $Cs_2V_5O_{13}$ ($\langle V\text{–}O\rangle$ = 2.05 Å), $K_2V_3O_8$ ($\langle V\text{–}O\rangle$ = 1.94 Å) in the vanadium bronzes ($\langle V\text{–}O\rangle$ = 1.90 Å), and in V_2O_5 ($\langle V\text{–}O\rangle$ = 1.89 Å). The smaller V–O distances observed for the vanadium bronzes and V_2O_5 result from the increase of the V(V) character. Moreover it is worth pointing out that the

TABLE IV

INTERATOMIC DISTANCES (Å) AND BOND ANGLES (°) IN THE PO_4 TETRAHEDRA

P(1)	O(2ii)	O(10)	O(14iii)	O(17)
O(2ii)	1.54(3)	2.50(3)	2.68(4)	2.44(5)
O(10)	113(2)	1.46(3)	2.52(3)	2.25(8)
O(14iii)	115(2)	109(1)	1.63(3)	2.69(8)
O(17)	104(2)	97(2)	116(2)	1.54(8)
P(2)	O(3ii)	O(8iv)	O(15v)	O(17)
O(3ii)	1.50(3)	2.56(3)	2.43(4)	2.54(6)
O(8iv)	115(2)	1.54(3)	2.43(3)	2.62(9)
O(15v)	113(2)	110(2)	1.42(3)	2.32(7)
O(17)	108(2)	111(2)	99(2)	1.63(8)
P(3)	O(4vi)	O(6)	O(11)	O(16)
O(4vi)	1.52(3)	2.49(4)	2.55(4)	2.31(4)
O(6)	109(2)	1.54(3)	2.45(4)	2.56(4)
O(11)	119(2)	112(2)	1.43(3)	2.45(4)
O(16)	96(1)	111(2)	109(1)	1.58(4)
P(4)	O(5vii)	O(7)	O(13viii)	O(16)
O(5vii)	1.52(3)	2.48(4)	2.44(4)	2.68(5)
O(7)	110(2)	1.51(4)	2.55(4)	2.56(4)
O(13viii)	103(2)	110(2)	1.61(3)	2.66(4)
O(16)	116(1)	108(2)	110(1)	1.64(4)

Note. Symmetry code. i: $-x, -y, z - 0.5$; ii: $0.5 - x, y - 0.5, z - 0.5$; iii: $0.5 + x, 0.5 - y, z$; iv: $x, y, z - 1$; v: $0.5 - x, 0.5 + y, z - 0.5$; vi: $-x, 1 - y, z - 0.5$; vii: $-x, 1 - y, z + 0.5$; viii: $-x, -y, z + 0.5$; ix: $x, y, z + 1$; x: $0.5 - x, y - 0.5, z + 0.5$.

coordination of vanadium in V_2O_5 and in the vanadium bronzes is in fact intermediate between a pyramid and an octahedron, so that their structure can also be described as the association of distorted octahedra (*23*).

The diphosphate groups exhibit an eclipsed configuration with P–O distances and O–P–O bond angles (Table IV) close to those generally observed in diphosphate compounds and especially in diphosphate tungsten bronzes (*24*). In particular it can be seen that the P–O distances corresponding to the bridging oxygen of P_2O_7 is higher than the other P–O bonds in agreement with the Brown theory (*25*).

In $K_2V_3P_4O_{17}$ the existence of $[VO_5]$ chains of corner-sharing VO_6 octahedra running along *c* (Fig. 2) is characteristically common in several V(V) and V(IV) phosphates. Such isolated ReO_3-type files are indeed observed in α-VPO_5 (Fig. 3a), VP_2SiO_9 (Fig. 4a), and VP_2O_7 (Fig. 5). $V_2P_2O_9$ also exhibits ReO_3-type chains of VO_6 octahedra (Fig. 6a), but contrary to the previous structures, the octahedral chains are not isolated: two ReO_3-type chains share the edge of their octahedra (Fig. 6a), forming double ReO_3-type files which are connected to each other through diphosphate groups (Fig. 6b). Infinite files of corner-sharing oc-

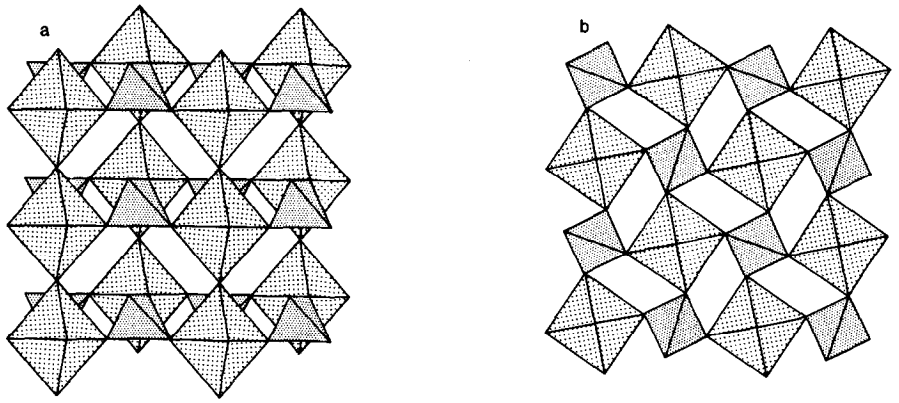

FIG. 3. The α-VPO_5 structure viewed: (a) along *a* showing the ReO_3-type files, (b) along *c* showing the connection between the files.

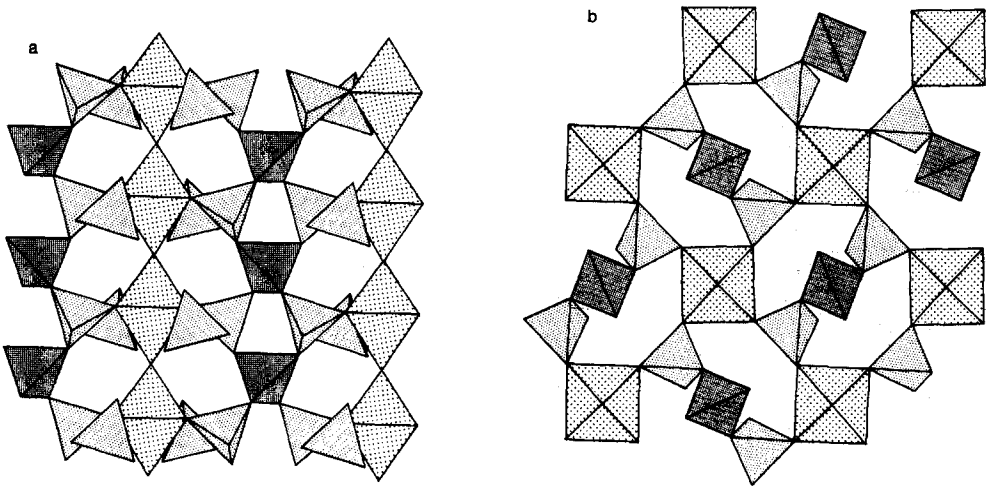

FIG. 4. Partial projection of the VP_2SiO_9 structure viewed: (a) along a showing the ReO_3-type files, (b) along c showing the connection between the files.

tahedra are also observed in β-VPO_5 (Fig. 7), as for $K_2V_3P_4O_{17}$. There chains are isolated from each other, but the O–O–O bond angle between two successive octahedra is close to 120° (or 60°) instead of 90° as in $K_2V_3P_4O_{17}$. Such files can be described as hexagonal tungsten bronze (HTB) type files. The adaptability of the diphosphate groups to the ReO_3-type files is a remarkable feature of the structure of $K_2V_3P_4O_{17}$. Each P_2O_7 group shares two corners with the $V(3)O_6$ octahedra, and each octahedron of the file shares the four corners of its basal plane, forming mixed chains $[V_2P_8O_{30}]_\infty$ running along c (Fig. 8). Such mixed chains can also be recognized in the structure of $V_2P_2O_9$ (Fig. 9). However, the $[V_2P_8O_{30}]_\infty$ chains do not exist as isolated files. Two such files are condensed by sharing the edges of the VO_6 and simultaneous elimination of two disphosphate groups leading to infinite chains $[V_4P_{12}O_{46}]_\infty$. This adaptability of the diphosphate groups to ReO_3-type files can be compared to that observed in the diphosphate tungsten bronzes $A_x(P_2O_4)_2(WO_3)_{2m}$ described by Labbe *et al.* (*26*). The structure of those latter bronzes is indeed described as ReO_3-type slabs connected through diphosphate planes. It is worth pointing out that the presence of diphosphate groups linked to ReO_3-type files is rather rare in the vanadophosphates. The analysis of the structure of VP_2O_7 shows that its ReO_3-type files are connected through infinite chains $[PO_3]_\infty$ of corner-sharing PO_4 tetrahedra (Fig. 5) whereas in the other vanadophosphates, the ReO_3-type files are connected to each other through single PO_4 tetrahedra. Moreover contrary

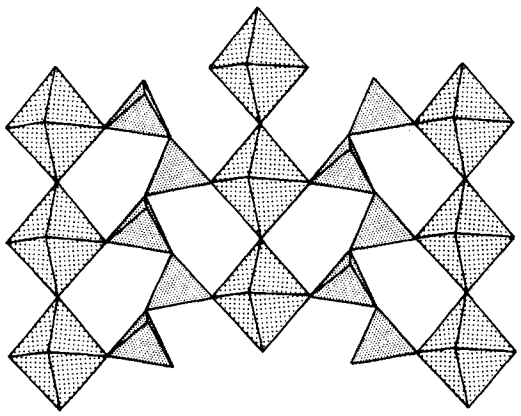

FIG. 5. The ReO_3-type files in VP_2O_7 and their connection by infinite chains of $[PO_3]_\infty$.

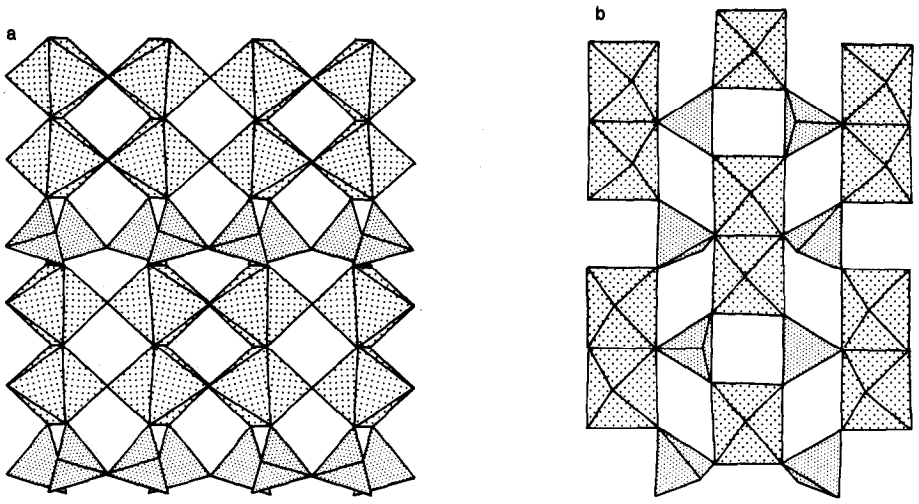

FIG. 6. $V_2P_2O_9$ structure viewed: (a) along the c axis, (b) along the a axis.

to $K_2V_3P_4O_{17}$ their structure is built up from mixed chains $[VPO_8]_\infty$ in which one tetrahedron alternates with one octahedron (Fig. 9a). In α-VPO_5 and β-VPO_5 such chains run along a (Fig. 3a) and b (Fig. 7a), respectively. In both compounds, each octahedron of a chain shares two opposite corners with one PO_4 tetrahedron of the adjacent chain, but the relative orientation of the chains in α-VPO_5 (Fig. 9b) is different from the one in β-VPO_5 (Fig. 9c).

The result is that the two other corners of each octahedron which are shared with another VO_6 octahedron of the adjacent chains form an ReO_3-type chain parallel to c in α-VPO_5 (Fig. 3b) and a HTB-type chain parallel to a in β-VPO_5 (Fig. 7b). The structure of $V_2P_2O_9$ is also built up from those mixed chains, which are associated in the (100) plane through the edges of their octahedra (Fig. 6b). Along a, the PO_4 tetrahedra

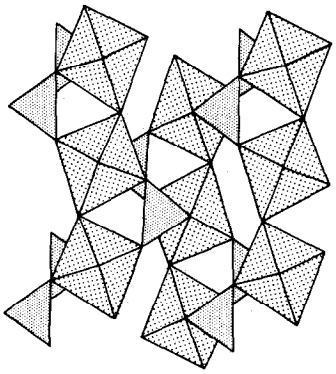

FIG. 7. Projection of the β-VPO_5 structure along b showing the HTB-type chains running along a.

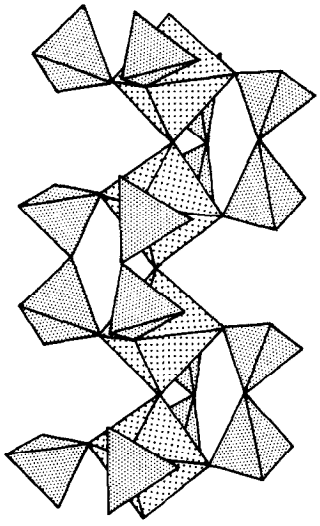

FIG. 8. $[V_2P_8O_{30}]_\infty$ chains running along c in $K_2(VO)_3(P_2O_7)_2$.

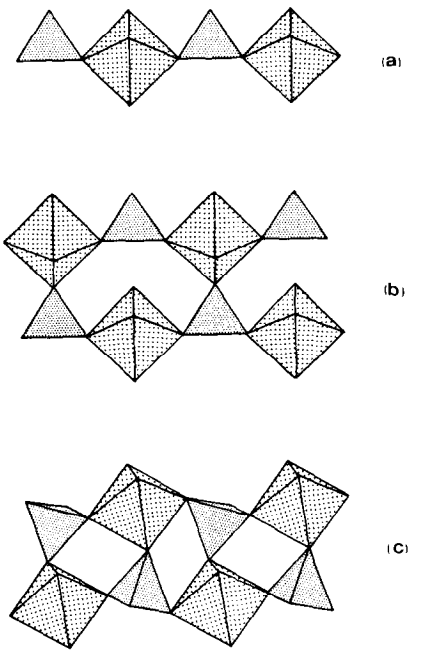

FIG. 9. (a) $[VPO_8]_\infty$ chain. Relative orientations of the $[VPO_8]_\infty$ chains in: (b) α-VPO_5, (c) β-VPO_5.

of each chain share their corners forming the P_2O_7 groups, whereas the VO_6 octahedra are also linked through their apices forming ReO_3-type chains (Fig. 6a). The structure of $VSiP_2O_9$ also shows the mixed chain $[VPO_8]_\infty$ formed from VO_6 octahedra and PO_4 tetrahedra running along the [110] direction (Fig. 4a), but in this case the orientations of the tetrahedron are different: two successive tetrahedra are in a trans position (Fig. 4b) while they are cis in the other oxides (Fig. 9a).

An interesting feature concerns the infinite ReO_3-type or HTB-type $[VO_5]_\infty$ file: in the same $[VO_5]_\infty$ file, the vanadium ions are all displaced from the barycenter in the same direction, forming a row of dipoles similar to those observed in ferroelectric oxides. Moreover, it is worth pointing out that in all those compounds the neighboring rows of dipoles point in opposite directions, leading to an antiferroelectric-type configuration. In this respect V(V), in spite of its d^0 configuration, differs from Nb(V) and Ti(IV) which exhibit several ferroelectric perovskites.

The host-lattice of $K_2V_3P_4O_{17}$ is also interesting by its particular character of intersecting-tunnel structure. The mixed chains $[V_2P_8O_{30}]_\infty$ are linked to each other through $[V_2O_{10}]$ units formed from one VO_5 pyramid and one VO_6 octahedron sharing one corner (Fig. 1). This framework delimits two types of tunnels running along the c axis, pseudo-rectangular tunnels similar to those observed in $P_8W_{12}O_{52}$ (*27*) and "snail-shell-shaped" tunnels which resemble the pseudo-hexagonal tunnels observed in Mo_5O_{14} (*28*).

Along the b axis, the observed tunnel (Fig. 2) results from the superposition of pentagonal rings (3 octahedra + 2 tetrahedra) and heptagonal rings (4 tetrahedra + 2 octahedra + 1 pyramid). The potassium ions K(1) belong to the "snail-shaped" tunnels whereas the cations K(2) are located at the intersection of the pseudo-rectangular tunnels and of the tunnels parallel to the b axis.

TABLE V

POTASSIUM–OXYGEN DISTANCES (Å)

K(1)–O(14^{viii})	= 2.66(3)
K(1)–O(15^{ix})	= 2.91(3)
K(1)–O(11^{ix})	= 2.97(3)
K(1)–O(8^{x})	= 2.99(3)
K(1)–O(13^{viii})	= 3.12(3)
K(1)–O(1^{x})	= 3.19(2)
K(1)–O(10^{x})	= 3.32(3)
K(1)–O(7)	= 3.33(4)
K(2)–O(4^{ii})	= 2.99(3)
K(2)–O(16^{iii})	= 3.00(2)
K(2)–O(17^{x})	= 3.10(2)
K(2)–O(9)	= 3.13(2)
K(2)–O(6^{x})	= 3.17(4)
K(2)–O(7^{ii})	= 3.18(4)
K(2)–O(10^{x})	= 3.28(3)

Note. See symmetry code in Table IV.

To determine the maximum bond length of the potassium atom to oxygen, the Donnay and Allman (*29*) procedure with the revised "Ionic radii" of Shannon (*30*) was used $K-O_{max} = 3.35$ Å. Accordingly each K(1) ion can be considered to be surrounded by eight oxygen atoms with K–O distances ranging from 2.66 to 3.33 Å (Table V). The mean K–O distance (2.94 Å) is a little greater than that deduced from the ionic radii (2.91 Å) of Shannon (*30*). Most striking is the K(2)–O bond lengths (Table V) which are all larger than 2.99 Å. The mean value of 3.12 Å is much greater than the sum of the ionic radii (2.86 Å). Such behavior suggests a possible mobility of the K ions which could account for their rather high isotropic thermal parameter ($B > 3$ Å^2). Thus, ion exchange properties of $K_2V_3P_4O_{17}$ should be investigated.

References

1. E. Bordes and P. Courtine, *J. Catal.* **57,** 236 (1979).
2. B. H. Wolf, N. Wustneck, M. Seeboth, V. M. Belousov, and V. A. Zazigalov, *Z. Chem.* **22,** 193 (1982).
3. A. Leclaire, H. Chahboun, D. Groult, and B. Raveau, *J. Solid State Chem.* **65,** 168 (1986).
4. E. Bordes, P. Courtine, and G. Pannetier, *Ann. Chim.* **8,** 105 (1983).
5. A. Leclaire, M. M. Borel, A. Grandin, and B. Raveau, *J. Solid State Chem.*, in press.
6. "International Tables for X-ray Cristallography," Vol. IV, Kynoch Press, Birmingham (Present distributor Reidel, Dordrecht) (1976).
7. C. E. Rice, W. R. Robinson, and B. C. Tofield, *Inorg. Chem.* **15**(2), 345 (1976).
8. J. M. Lango and P. Kierkegaard, *Acta Chem. Scand.* **9,** 1906 (1965).
9. A. Erragh, Thesis, University of Bordeaux (1986).
10. J. M. Lango, and R. J. Arnott, *J. Solid State Chem.* **1,** 394 (1970).
11. H. A. Eick and L. Kihlborg, *Acta Chem. Scand.* **20**(3), 729 (1966).
12. Y. E. Gorbunova and C. A. Linde, *Dokl. Akad. Nausk SSSR* **245,** 584 (1978).
13. P. Kierkegaard and M. Westerlund, *Acta Chem. Scand.* **18,** (10), 2217 (1964).
14. A. Leclaire, J. C. Monier, and B. Raveau, *J. Solid State Chem.* **48,** 147 (1983).
15. B. Jordan and C. Calvo, *Canad. J. Chem.* **51,** 2621 (1973).
16. R. Gopal and C. Calvo, *J. Solid State Chem.* **5,** 432 (1972).
17. N. Middlemiss, Ph. D. thesis, MacMaster University, Canada (1978).
18. K. Waltersson and B. Forslund, *Acta Crystallogr. B* **33,** 784 (1977).
19. J. Galy and A. Carpy, *Acta Crystallogr. B* **31,** 1794 (1975).
20. P. Hagenmuller, "Comprehensive Inorganic Chemistry" (A. F. Trotman-Dickenson, Ed.), Pergamon, New York (1973).
21. A. D. Wadsley, *Acta Crystallogr.* **10,** 261 (1957).
22. H. G. Bachmann, F. R. Ahmed, and W. Z. Barnes, *Z. Kristallogr.* **115,** 110 (1961).
23. B. Raveau, *Rev. Inorg. Chem.*, **9,** 37 (1987).
24. B. Raveau, *Proc. Indian Acad. Sci.* (*Chem. Sci.*) **96,** 419, 448 (1986).
25. I. D. Brown and K. K. Wu, *Acta Crystallogr. B* **32,** 1957 (1976).
26. Ph. Labbe, D. Ouachee, M. Goreaud, and B. Raveau, *J. Solid State Chem.* **50,** 163 (1983).
27. B. Domenges, M. Goreaud, Ph. Labbe, and B. Raveau, *Acta Crystallogr. B* **38,** 1724 (1982).
28. L. Kihlborg, *Acta Chem. Scand.* **13,** 954 (1959).
29. G. Donnay and R. Allman, *Amer. Mineral.* **55,** 1003 (1970).
30. R. D. Shannon, *Acta Crystallogr. A* **32,** 751 (1976).